Application of direct-fitting, mass integral, and multirate methods to analysis of flowing fluid electric conductivity logs from Horonobe, Japan

Christine Doughty,[1] Chin-Fu Tsang,[1] Koichiro Hatanaka,[2] Satoshi Yabuuchi,[2] and Hiroshi Kurikami[2,3]

Received 15 August 2007; revised 11 March 2008; accepted 29 May 2008; published 2 August 2008.

[1] The flowing fluid electric conductivity (FFEC) logging method is an efficient way to provide information on the depths, salinities, and inflow strengths of individual conductive features intercepted by a borehole, without the use of specialized probes. Using it in a multiple-flow rate mode allows, in addition, an estimate of the transmissivities and inherent (far-field) hydraulic heads in each of the conductive features. The multirate method was successfully applied to a 500-m borehole in a granitic formation and reported recently. The present paper describes the application of the method to two zones within a 1000-m borehole in sedimentary rock, which produced, for each zone, three sets of logs at different pumping rates, each set measured over a period of about 1 day. The data sets involve several complications, such as variable well diameter, gradual water level decline in the well during logging, possible fluid flow through the unfractured rock matrix, and effects of drilling mud. Various techniques were applied to analyze the FFEC logs: direct-fitting, mass integral, and the multirate method mentioned above. In spite of complications associated with the tests, analysis was able to identify 44 hydraulically conducting fractures distributed over the depth interval 150–775 m below ground surface. The salinities (in FEC), and transmissivities and hydraulic heads (in dimensionless form) of these 44 features were obtained and found to vary significantly among one another. These results were compared with transmissivity and head values inferred from eight packer tests that were conducted in this borehole over the same depth interval. FFEC results were found to be consistent with packer test results, thus demonstrating the robustness of the FFEC logging method under nonideal conditions.

Citation: Doughty, C., C.-F. Tsang, K. Hatanaka, S. Yabuuchi, and H. Kurikami (2008), Application of direct-fitting, mass integral, and multirate methods to analysis of flowing fluid electric conductivity logs from Horonobe, Japan, *Water Resour. Res.*, *44*, W08403, doi:10.1029/2007WR006441.

1. Introduction

[2] Knowledge of the locations and hydraulic properties of conductive features is needed to understand flow and transport through fractured rocks, which is required for a variety of practical applications, including geologic storage of nuclear waste, toxic chemicals and carbon dioxide, and exploitation of natural resources such as petroleum and geothermal fluids. Boreholes drilled deep into the rock are often used to obtain this information. Various downhole methods for studying fracture flow have been developed over the past few decades. Coring and geophysical methods may be able to locate the fractures, but they are unlikely to provide direct information on fracture flow properties. Straddle-packer pump testing yields fracture flow properties, but it is very time consuming and expensive. Flow-logging techniques are an attractive alternative: They measure flow directly and are efficient to deploy in the field. Several varieties of flow logging exist, including spinner surveys [*Molz et al.*, 1989], heat pulse flowmeters [*Paillet and Pedler*, 1996; *Paillet*, 1998; *Öhberg and Rouhiainen*, 2000], tracer dilution analysis [*Brainerd and Robbins*, 2004], and the flowing fluid electric conductivity (FFEC) logging method, sometimes referred to as hydrophysical logging, the technique used in the present study.

[3] To initiate the FFEC logging method, wellbore fluid is replaced with water of constant salinity different from that of the formation water, a process known as recirculation. Then FEC profiles in the wellbore are measured at a series of times while the well is pumped at a constant rate. Locations where native fluid enters the wellbore show peaks in the FFEC logs. By fitting the growth and movement of these peaks with a numerical model, one can infer inflow strengths and salinities of individual permeable features intersected by the borehole. Since *Tsang et al.* [1990] introduced the method, it has been widely applied in deep wells down to 1500 m or more [*Kelley et al.*, 1991; *Guyonnet et al.*, 1993; *Doughty et al.*, 2005], in inclined

[1] Earth Sciences Division, Lawrence Berkeley National Laboratory, Berkeley, California, USA.
[2] Horonobe Underground Research Unit, Japan Atomic Energy Agency, Hokkaido, Japan.
[3] Now at Nuclear Waste Management Organization of Japan, Tokyo, Japan.

0043-1397/08/2007WR006441$09.00

boreholes drilled in the underground Grimsel Test Laboratory [*Marschall and Vomvoris*, 1995], and extensively in shallower wells down to about 100 m [*Evans et al.*, 1992; *Pedler et al.*, 1992; *Bauer and LoCoco*, 1996; *Paillet and Pedler*, 1996; *Karasaki et al.*, 2000]. Continued development of analytical and numerical data analysis techniques [*Löw et al.*, 1994; *Evans*, 1995; *Tsang and Doughty*, 2003; *Doughty and Tsang*, 2005] have broadened the range of applicability and enhanced the ease of use of the method. Note that FFEC logging requires little or no specialized equipment or expertise, and may be carried out more quickly than most other methods, making it a valuable tool for efficient subsurface characterization.

[4] Data analysis techniques include three main methods: (1) direct fitting of the time series of FFEC profiles, which yields the locations, inflow strengths, and salinities of permeable features [*Tsang et al.*, 1990]; (2) the mass integral method, in which each FFEC profile is integrated over the entire logged interval to provide an estimate of salt mass in place as a function of time [*Doughty and Tsang*, 2005]; and (3) multirate FFEC logging, in which FFEC logging is repeated using two different well-pumping rates, which enables the transmissivities and inherent (far-field) hydraulic heads of the different permeable features to be determined [*Tsang and Doughty*, 2003]. Using multiple pumping rates to infer transmissivity and inherent hydraulic head of individual fractures has also been investigated in conjunction with use of a heat pulse flowmeter [*Paillet*, 1998, 2000] and tracer dilution analysis [*Brainerd and Robbins*, 2004].

[5] Direct-fitting and multirate analyses for FFEC logging were recently carried out successfully for a 500-m-deep borehole in fractured granitic rock in the Tono region of Japan [*Doughty et al.*, 2005]. The analyses identified 19 hydraulically conducting fractures, which showed a range of values for transmissivity, salinity, and hydraulic head. FFEC results compared well with static FEC profiles and independent chemical, geological, and hydrogeological data. The present paper describes a field application of the multirate FFEC logging method, using data from a 1000-m-deep well known as Well HDB-11, in fractured sedimentary rock in the Horonobe area of Japan. This case differs from the Tono application [*Doughty et al.*, 2005] in several significant ways. Not only is the rock sedimentary instead of granitic, but also a number of complications are associated with the logging data, including (1) a section of the borehole having a variable wellbore diameter; (2) the presence of a free water surface in the borehole (i.e., the logged zone is not isolated with packers); (3) flow of low-salinity water into fractures during the initial recirculation period; (4) periods of unknown pumping rate during FFEC logging; (5) a small increase in salinity all along the borehole during FFEC logging, possibly arising from flow through the unfractured rock matrix itself or the diffusion of salt from residual mud used in drilling the well; (6) a gradual borehole water level decline during FFEC logging; (7) possible unknown inflows into the borehole from unmonitored borehole sections; and (8) sets of FFEC profiles that are not all internally consistent. Whereas the Tono application demonstrated the first field application of the multirate FFEC logging method, the Horonobe application examines the robustness of the method under nonideal conditions.

2. Methodology

[6] This section gives a summary of data collection and analysis methods. Details of the data collection method are given by *Doughty et al.* [2005]. Details of the analysis method are given by *Tsang et al.* [1990], *Tsang and Doughty* [2003], *Doughty and Tsang* [2005], and *Doughty et al.* [2005].

2.1. Data Collection

[7] In the FFEC logging method, the wellbore water is first replaced by water of a constant salinity different from that of the formation water, a process known as recirculation. Deionization of native water is one convenient means to produce replacement water with a salinity contrast, but shallow groundwater may also be used if it has a salinity distinct from that of the formation of interest. For simplicity, replacement water is always referred to as deionized (DI) water below. Recirculation is done by injecting DI water through a tube to the bottom of the wellbore at a low rate, while simultaneously pumping from the top of the well at the same rate. The goal is to completely replace the wellbore water with DI water without altering wellbore hydraulic head, so that no DI water is pushed out into the formation or is any formation water pulled into the well. The FEC of the effluent is monitored throughout the recirculation period, which continues until a low stable FEC value is reached. If the final, stable, effluent FEC is substantially higher than the DI water FEC, it indicates that native fluid is entering the wellbore during recirculation. This may occur because wellbore hydraulic head was unintentionally dropped during recirculation. It can also occur if different permeable features intercepted by the wellbore have different inherent hydraulic heads, which sets up an unavoidable internal wellbore flow, with formation water entering the wellbore through features with higher hydraulic head and DI water entering the formation through features with lower hydraulic head.

[8] Next, the well is shut in (i.e., injection and pumping are stopped) and the DI water tube is removed. Then the well is pumped from the top at a constant low flow rate Q_1 (e.g., several or tens of liters per minute), while an electric conductivity probe is lowered into the wellbore to scan the FEC as a function of depth. This produces what is known as a flowing FEC (or FFEC) log or profile. With constant pumping conditions, a series of five or six FFEC logs are typically obtained over a 1- or 2-day period. Optionally, the entire procedure may be repeated using a different pumping rate Q_2, typically half or double the original rate Q_1. Throughout the process, the water level in the well should be monitored.

2.2. Data Analysis

[9] At depth locations where native water enters the wellbore (inflow feed points), the FFEC logs display peaks. These peaks grow with time and are skewed in the direction of water flow. By analyzing these logs as described below, it is possible to obtain the inflow rates and salinities of groundwater inflow from the individual feed points. Although locations where water leaves the wellbore (outflow feed points) do not produce distinct peaks in the FFEC

logs, they can sometimes be identified by their impact on other peaks using a mass integral method [*Doughty and Tsang*, 2005]. By performing FFEC logging using different pumping rates, a procedure called multirate FFEC logging [*Tsang and Doughty*, 2003], the transmissivities and inherent hydraulic heads of the permeable features giving rise to the feed points can also be determined.

[10] The numerical models BORE [*Hale and Tsang*, 1988] and the enhanced version BORE II [*Doughty and Tsang*, 2000] calculate the time evolution of ion concentration (salinity) in the wellbore during FFEC logging by solving the one-dimensional advection-dispersion equation, given a pumping rate Q and a set of feed point locations z_i, strengths q_i, and salinities C_i (i.e., the forward problem). Fluid flow in the wellbore is considered quasi steady; that is, fluid is assumed to be incompressible so it responds instantly to changes in pumping rate or feed point strength. Internal wellbore flow occurring during recirculation results in nonuniform salinity along the borehole, which may be accounted for in two ways. First, a nonuniform conductivity profile $C_0(z)$ may be specified as the initial condition for the model. Second, a starting time t_{0i} may be specified for each feed point, to indicate the time after which fluid entering the wellbore has salinity C_i, to reflect DI water that entered the formation during recirculation. Density differences between the original wellbore fluid (DI or low-salinity water, which may contain traces of drilling mud) and formation fluid flowing into the wellbore are neglected. Another version of the code, VHBORE [*Hale and Tsang*, 1994], does consider compressible flow with compositional density differences, but it is not used here. The governing equations for BORE II are presented by *Doughty and Tsang* [2005].

[11] The general procedure for using BORE II is to assign feed point locations z_i by identifying individual peaks in the early time FFEC profiles, then to assign feed point properties (q_i, C_i, and t_{0i}) by trial and error until an acceptable match between modeled and observed FFEC profiles is obtained (i.e., an inverse problem). This procedure is known as direct fitting. Integrating the FFEC profiles over the entire logged interval or a desired subinterval (the mass integral method) provides an estimate of salt mass in the borehole interval under study as a function of time, which provides a useful constraint for the analysis. If FFEC logs were only collected using one pumping rate Q, then the analysis would end here.

[12] However, if multiple sets of FFEC logs were collected using different pumping rates Q, then the inverse procedure is repeated for each value of Q, with the inverse problems constrained by requiring that the same set of z_i and C_i values be used for each one. Assuming that two sets of FFEC logs were collected with pumping rates Q_1 and Q_2, and that the strengths of individual feed points i, as evaluated by BORE II, are $q_i^{(1)}$ and $q_i^{(2)}$ respectively, then *Tsang and Doughty* [2003] and *Doughty and Tsang* [2005] showed that

$$\frac{T_i}{T_{\text{tot}}} = \frac{q_i^{(1)} - q_i^{(2)}}{Q_1 - Q_2} \tag{1}$$

$$I\Delta P_i = \left(\frac{q_i^{(1)}/Q_1}{T_i/T_{\text{tot}}} - 1 \right) Q_1, \tag{2}$$

where T_i/T_{tot} is the fraction of the total transmissivity of the logged interval corresponding to the fracture or permeable zone represented by the ith feed point ($\Sigma T_i/T_{\text{tot}} = 1$) and $\Delta P_i = P_i - P_{\text{avg}}$ where P_i is the inherent hydraulic head of fracture i and P_{avg} is the stabilized hydraulic head in the wellbore when it is shut-in for an extended time. I is a ratio known as the productivity index (in the petroleum literature) or specific capacity (in hydrology), which is defined as the ratio of pumping rate to steady state drawdown during a well test. I characterizes the entire permeable formation intersected by the wellbore in an average sense under steady state flow conditions. In the FFEC context, we may approximate I as

$$I = \frac{Q_1}{P_{\text{avg}} - P_{wb}^{(1)}}, \tag{3}$$

where $P_{wb}^{(1)}$ is the hydraulic head in the wellbore (presumed constant) during the FFEC logging at $Q = Q_1$.

[13] The derivation of equations (1) and (2) assumes that the flow geometries within all the hydraulically conductive fractures intersecting the borehole are the same (e.g., all radial flow or all linear flow). The inherent (also known as far-field) hydraulic head P_i is the ambient or undisturbed hydraulic head in a fracture (or permeable layer) that the borehole intersects, and it is the value that would be measured under nonpumping conditions with packers inflated in the wellbore on either side of the fracture to isolate it for a substantial time period to attain steady state pressure conditions. In contrast, P_{avg} is the value that would be measured under nonpumping conditions when the wellbore has been open to all feed points in the logged interval for a substantial time period. P_{avg} can be calculated as a transmissivity-weighted average over all P_i values: $P_{\text{avg}} = \Sigma(T_i P_i)/T_{\text{tot}}$. The head difference $\Delta P_i = P_i - P_{\text{avg}}$ provides a measure of the driving force for fluid flow between hydraulically conducting fractures and the wellbore under nonpumping or shut-in conditions, which gives rise to internal wellbore flow. Note that from the definition of P_{avg} above, if all the P_i values are the same, then $P_i = P_{\text{avg}}$, so that all $\Delta P_i = 0$, and there will be no internal wellbore flow under nonpumping conditions. In this case, equation (2) shows that feed point strength q_i is proportional to fracture transmissivity T_i, making it possible to determine T_i/T_{tot} by matching FFEC profiles for just one pumping rate Q.

[14] The quantities on the left-hand sides of equations (1) and (2) are the fundamental results of a multirate analysis, and they depend only on the q_i values obtained by matching FFEC logs for various Q values. If T_{tot}, I, and P_{avg} are also known (e.g., from a conventional well test of the entire well section), then the T_i and P_i values themselves can be directly calculated from these two equations. Additionally, because T_i and P_i appear in ratios in equations (1) and (2), if one particular set of T_j and P_j are measured (e.g., from a well test on a packed-off interval across fracture j), then all the additional T_i and P_i values can also be determined.

[15] The multirate analysis requires two sets of FFEC logs at two pumping rates (at Q and $2Q$, for example), but if three sets of logs for three pumping rates, Q_1, Q_2, and Q_3, are available, then three sets of results can be obtained by analyzing three combinations of data sets: (Q_1 and Q_2), (Q_2

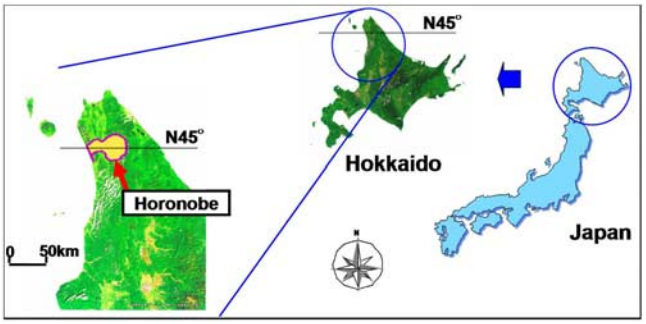

Figure 1. Location map of Horonobe.

and Q_3), and (Q_3 and Q_1). This permits internal checking, a means to evaluate measurement errors, and an estimate on the confidence level of the analysis results. One interesting option (not considered here) is to use $Q = 0$ for the first pumping rate, which has the advantage of investigating internal flow directly. If one logs at $Q_1 = 0$ and no peaks develop, then it immediately follows that there is no internal wellbore flow, and consequently that all P_i are the same. Then equation (1) may be used while logging at some $Q_2 > 0$ to determine T_i/T_{tot} (a procedure first suggested by *Molz et al.* [1989]). The disadvantage of logging with $Q = 0$ is that if there is internal flow, half the flow will be outflow, which is usually invisible on a FFEC profile, and hence much more difficult to analyze [*Doughty and Tsang*, 2005; *Doughty et al.*, 2005].

3. Horonobe Well HDB-11 Data

[16] Horonobe, located in the northernmost part of Hokkaido, Japan (Figure 1), is the site of an underground research laboratory (URL), where hydrogeochemical investigations are being conducted to develop technologies and methodologies that may in the future be applied during the geological disposal of high-level radioactive waste in sedimentary rock in Japan [*Hama et al.*, 2007]. The main subsurface investigation area is about 3 km × 3 km square, including the URL construction site, which is located about 15 km east of the present coastline of the Japan Sea. The gentle topography in the study area is thought to be a periglacial landform. Horonobe overlies Neogene sedimentary sequences (in ascending order, Souya coal-bearing Formation, Masuhoro Formation, Wakkanai Formation, Koetoi Formation, and Yuchi Formation), which are underlain by an igneous and Palaeogene-to-Cretaceous sedimentary basement. The Wakkanai and Koetoi formations, composed of Neogene argillaceous sedimentary rocks, are intercepted by Well HDB-11 and are also the host rocks for the URL.

[17] Hydrologic properties reported for the URL host rocks [*Hama et al.*, 2007] include porosities up to 60% and hydraulic conductivities ranging from 2×10^{-9} to 4×10^{-8} m/s for the Koetoi Formation, and porosities of 30–40% and hydraulic conductivities ranging from 3×10^{-10} to 8×10^{-9} m/s for the deeper Wakkanai Formation. Hydraulic conductivity of the intact diatomaceous mudstone has been reported to be as low as 10^{-13}–10^{-11} m/s [*Shigeta et al.*, 2003], and thus the larger observed values of hydraulic conductivity are attributed to fluid flow through fractures or fracture zones.

[18] The area is tectonically active, and microearthquake swarms have occasionally occurred in and around Horonobe. The eastern margin of the Japan Sea is a well-defined seismic zone, especially for microearthquakes. The Omagari Fault, a NW-SE trending fault with surface trace inferred to be about 1 km east of Well HDB-11, was active until early Quaternary times and is believed to have a maximum vertical displacement of over 1000 m. Present-day active faults are thought to occur to the west of the Omagari Fault. In addition, historical coal mines were present in Horonobe, and oil/gas exploration work (including deep borehole investigations) has been conducted in the region. Further details of the Horonobe URL site are given by *Hama et al.* [2007].

[19] Well HDB-11 was drilled in four stages. FFEC logs were taken after the second stage of drilling from 150 to 450 m through the Koetoi Formation (hereinafter denoted the shallow zone), and after the third stage of drilling from 450 to 800 m through the Wakkanai Formation (hereinafter denoted the deep zone). During logging of each zone, the well was cased from the surface to the top of the logged zone, leaving the logged zone uncased.

[20] Figure 2 shows the caliper log for Well HDB-11. Over the depth interval of the shallow zone (Koetoi Formation, 150–450 m below ground surface (bgs)) the wellbore diameter is nearly constant at 164 mm. Over the depth interval of the deep zone (Wakkanai Formation, 450–800 m bgs) the wellbore diameter is more variable: Below 550 m depth, it is nearly constant at 162 mm, but above 550 m it gradually increases to 240 mm. This diameter increase will cause peaks in FFEC profiles to move upward more slowly. Thus if the change in borehole diameter is not accounted for, data analysis will result in feed point strengths that are underestimated over the depth interval 450–550 m.

[21] FFEC logging was repeated three times for both the shallow and deep zones, using different pumping rates, for a total of six tests. Prior to each logging period, recirculation occurred, in which groundwater with very low electrical conductivity (9 mS/m) was pumped from a nearby shallow well and injected into Well HDB-11 just below the bottom of the zone to be logged (10–15 m above the bottom of the well), while water was simultaneously pumped out of the top of the well at the same rate, using a submersible pump located near the ground surface. The total volume of water

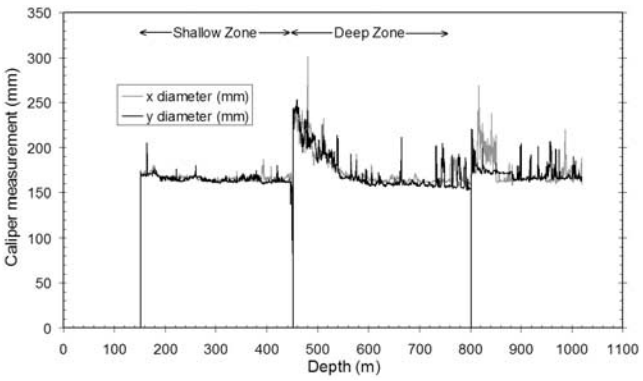

Figure 2. Caliper log for Well HDB-11.

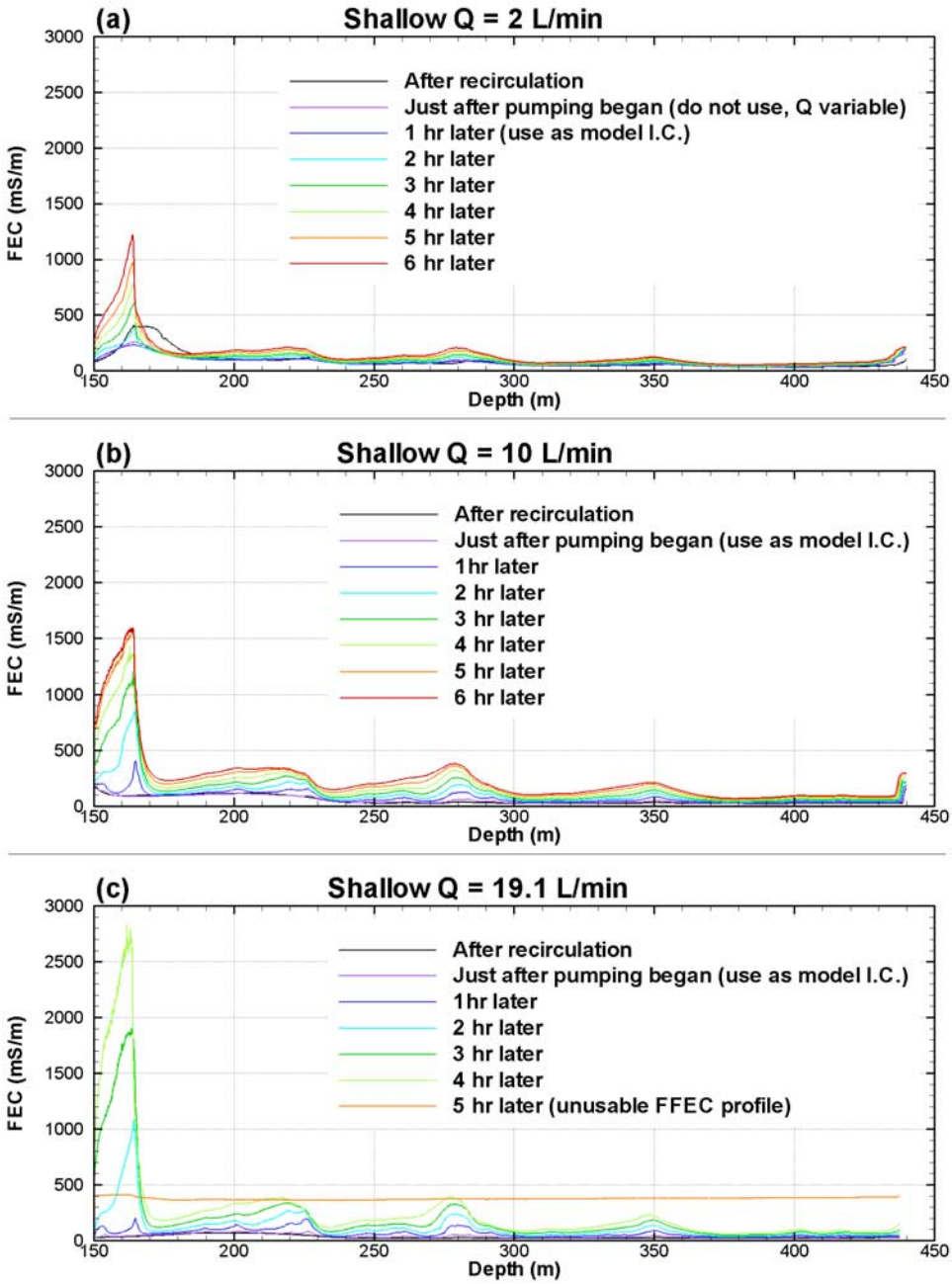

Figure 3. Original flowing fluid electric conductivity (FFEC) data for shallow zone.

replaced during each recirculation period was 1.5 to 4 times the borehole volume. By the end of each recirculation period, the electric conductivity of the effluent had stabilized at less than 40 mS/m. There was a short quiescent period between recirculation and logging during which the well was shut in. Then, during the logging periods, water was pumped out of the top of the well using the same submersible pump used during recirculation.

[22] For the three shallow-zone tests, logging was conducted using pumping rates of 2 L/min, 10 L/min, and 19.1 L/min. Figure 3 shows the resulting FFEC profiles, and Figure 4 shows water level versus time for each test. For the three deep-zone tests, logging was conducted using pumping rates of 5 L/min, 10 L/min, and 15 L/min. Figure 5 shows the resulting FFEC profiles, and Figure 6 shows water level versus time for each test.

[23] Visual examination of the FFEC profiles (Figure 3 and Figure 5) indicates that not all the profiles can be used for analysis. In some cases it appears that the tool that measures fluid electric conductivity did not function at all (e.g., Figure 3, Q = 19.1 L/min, 5-h profile). In other cases, the results look qualitatively correct, but the profiles appear shifted with depth or otherwise distorted (e.g., Figure 5, Q = 5 L/min, 4- and 5-h profiles), suggesting that the tool did not move freely through the wellbore. Subsequent analysis suggested that the problems were caused by slime (muddy water used in drilling) adhering to the sensor. A total of seven FFEC profiles obtained during the six tests

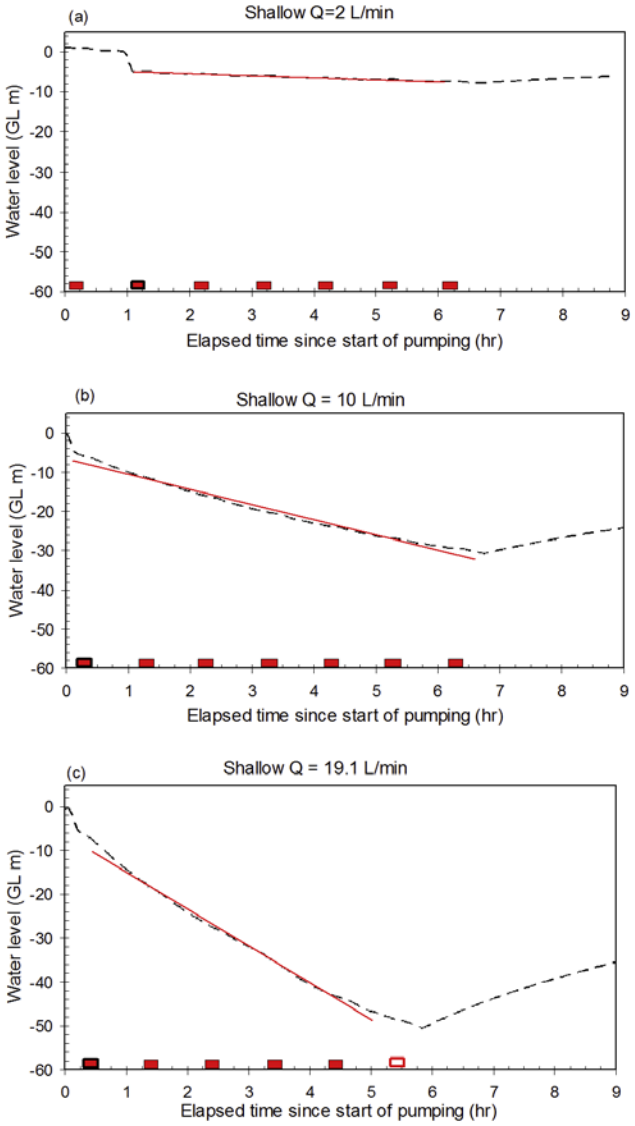

Figure 4. Water level data obtained during FFEC logging of shallow zone (dashed curve) and linear fit of the portion of the curve obtained while usable FFEC logs were collected (solid line). The early time sharp drop in water level is associated with a short-term increase in pumping rate. Times at which FFEC logging occurred are shown as boxes. The black-outlined box identifies the profile used as the initial condition for the BORE II model. The open box indicates an FFEC profile that could not be used for analysis.

were not included in the analysis because the FFEC profiles were not internally consistent with the remainder of the profiles; they are identified as "unusable FFEC profile" in Figure 3 and Figure 5.

[24] The FFEC profiles collected at the end of the recirculation periods (the earliest profiles in Figure 3 and Figure 5) exhibited only small peaks, consistent with the low effluent FEC, indicating that little internal wellbore flow occurred during recirculation. This in turn suggests that there is little difference among the inherent hydraulic head values of the permeable features, and according to equation (2), that variations in inflow strength q_i primarily reflect variations in transmissivity T_i.

[25] Water level data (Figure 4 and Figure 6) were collected during the FFEC logging periods. For the shallow-zone tests, pumping rate increased by an unknown amount for a short period of time early in the tests, then returned to its specified value. The water level in the wellbore dropped sharply during the high pumping-rate period, then declined at a nearly linear rate in response to the constant pumping rate (Figure 4). For the deep-zone tests, water level also dropped sharply during the first few minutes of the test, followed by a more gradual decline (Figure 6). The gradual decline of the deep-zone tests was less linear than for the shallow-zone tests, showing a decreasing rate of water level change. The times at which FFEC logs were collected are also shown in Figure 4 and Figure 6.

[26] Ideally, one would use the water level data obtained during logging (Figure 4 and Figure 6) as an open-hole well test to determine T_{tot}, I, and P_{avg}, the properties of the entire interval of the borehole being logged, as described above in section 2.2. This cannot be done with confidence in the present case because we do not know either the entire pumping-rate history during the logging period, due to the early time unknown increase in pumping rate, or the complete drawdown record, due to the slow hydrologic response time of the system.

[27] Moreover, because the water level declined throughout the logging period, we could not assume that the pumping rate during logging Q equaled the total flow out of the formation, denoted Q_{form}. Therefore we assumed that pumping rate Q is the sum of two terms $Q = Q_{wb} + Q_{form}$, where Q_{wb} is water removed from the wellbore as the water level in the well declined. Q_{wb} can be estimated by multiplying the rate at which water level declined by the cross-sectional area of the wellbore at the depth of the water level. A linear decline in water level corresponds to a constant value of Q_{wb}, and coupled with a constant value of Q, implies that Q_{form} is also constant, which greatly simplifies the BORE II analysis. For the shallow-zone tests, Q_{wb} was reasonably constant, suggesting that for time periods when Q was constant, treating Q_{form} as a constant would be a reasonable assumption. Therefore the BORE II analysis did not attempt to match logs collected during the initial period of high pumping rate; instead, the first FFEC profile collected after Q became constant was used as the model initial condition. In contrast, for the deep-zone tests, Q_{wb} continued to decrease with time after Q became constant, and thus only the logs collected while the water level decline was approximately linear were matched, with the first FFEC profile collected after Q_{form} became constant used as the model initial condition. The FFEC logs that were not analyzed because Q_{form} could not be assumed constant are identified in Figure 5. Table 1 summarizes the Q, Q_{wb}, and Q_{form} values assumed for the tests, with Q_{wb} determined from the slope of the linear fits to water level versus time data shown in Figure 4 and Figure 6.

[28] The presence of drilling mud in the wellbore may affect fluid logging two ways: through its salinity and its density. Possible salinity effects are described in section 4 below. Density effects were neglected in the analysis, because although the drilling mud itself is presumably significantly denser than formation fluid, most of the mud

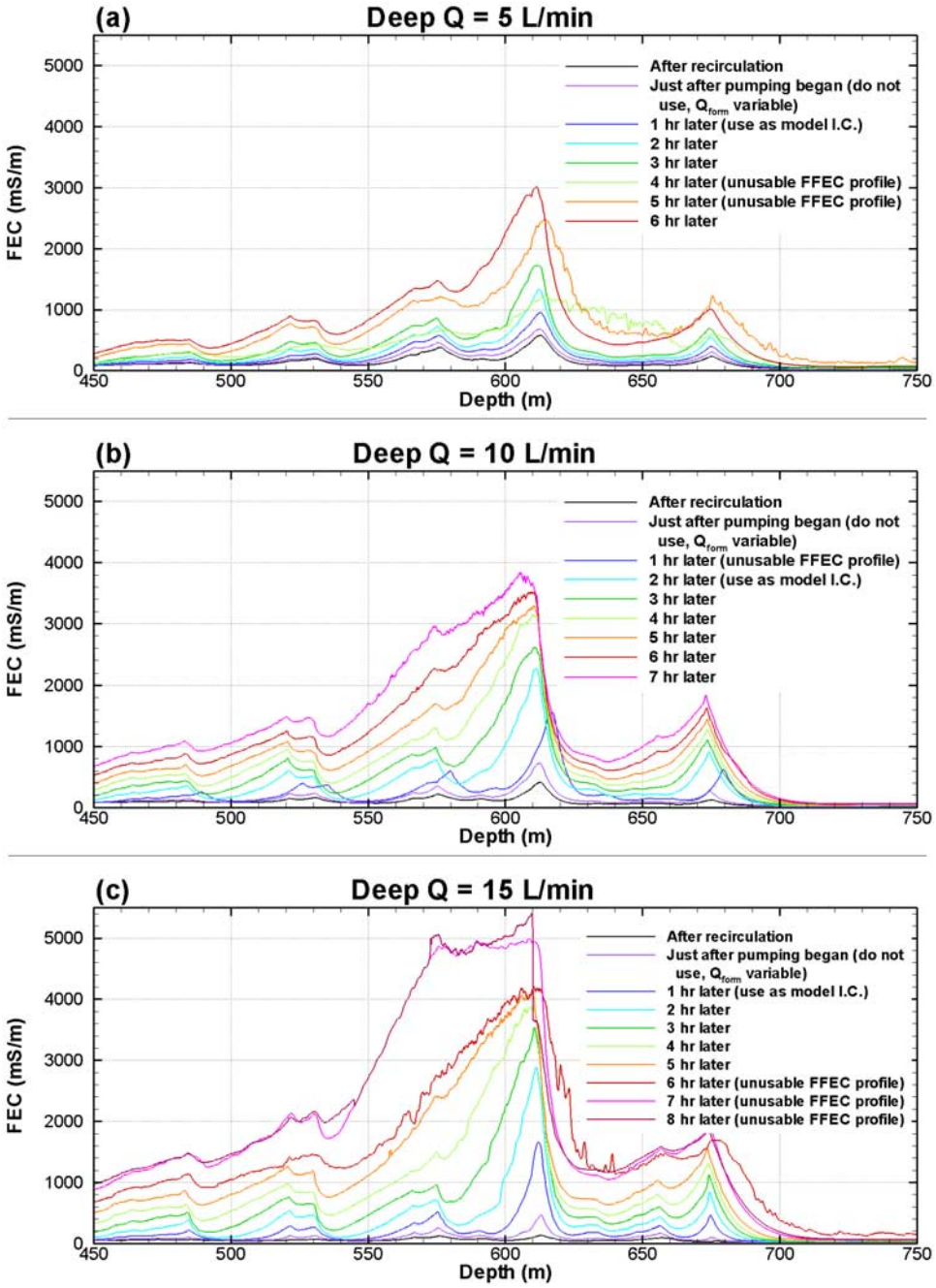

Figure 5. Original FFEC data for deep zone.

should be flushed out of the wellbore during the initial recirculation period.

[29] In Well HDB-11, the borehole temperature varies from 11° to 27°C over the depth range of FFEC logging. Prior to analyzing the FFEC logs with BORE II, the FEC values obtained in the field were temperature-corrected using the relationship [*Schlumberger, Ltd.*, 1984] $\mathrm{FEC}(20°\mathrm{C}) = \mathrm{FEC}(T)/[1 + S(T - 20°\mathrm{C})]$, with $S = 0.024°\mathrm{C}^{-1}$. This correction is required because BORE II assumes a constant temperature of 20°C.

[30] Typically during FFEC logging, electric conductivity in mS/m or μS/cm is converted to salinity in g/L, using a quadratic relationship developed by *Hale and Tsang* [1988]. However, for the present study, FEC values were above the range of applicability of the relation. Therefore no unit conversion was made and salinities C_i are presented in electric conductivity units mS/m.

4. Analysis of Shallow FFEC Logs

[31] The numerical model BORE II [*Doughty and Tsang*, 2000] was used to analyze the three sets of shallow-zone FFEC logs for three pumping rates $Q = 2$ L/min, 10 L/min, and 19.1 L/min, to obtain a set of inflow locations z_i, feed point strengths q_i, and salinities C_i. First, the z_i values were obtained by visually examining early time FFEC logs obtained in the field, before individual peaks begin to interfere with each other. Generally, the z_i were easy to

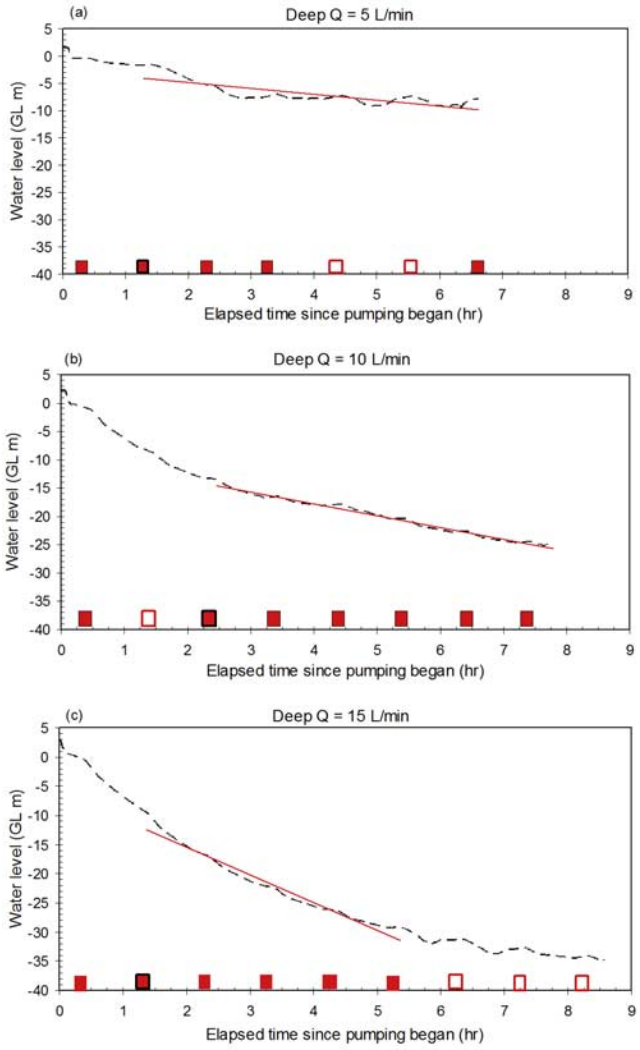

Figure 6. Water level data obtained during FFEC logging of deep zone (dashed curve) and linear fit of the portion of the curve obtained while usable FFEC logs were collected (solid line). The early time sharp drop in water level is associated with a short-term increase in pumping rate. Times at which FFEC logging occurred are shown as boxes. The black-outlined box identifies the profile used as the initial condition for the BORE II model. The open boxes indicate FFEC profiles that could not be used for analysis.

determine with good accuracy. Given the inflow locations z_i, the matching process was then conducted by using BORE II to model FFEC profiles with feed point strengths q_i and salinities C_i chosen by trial and error, in order to produce the best match to the FFEC logs obtained in the field. The C_i values for different depths z_i could vary among one another, but each C_i was maintained the same for all three data sets with different pumping rates. The feed point strengths q_i were allowed to be different for different z_i and for the different pumping rates.

[32] The matching made use of the following facts: The area under an isolated FEC peak is proportional to the product q_iC_i, the speed of a peak moving up the wellbore depends only on the sum of q_i values for the current and deeper peaks, and the steady state height of the deepest peak depends only on C_i. The initial trial considered the C_i to be the same for all inflow points (corresponding to 1000 mS/m), but this restriction was relaxed as needed to improve the match. At the early stages of the fitting process, each test was treated individually. Later, the q_i values for all three tests were varied concurrently, using equations (1) and (2) to constrain possible values of $q_i^{(1)}$, $q_i^{(2)}$, and $q_i^{(3)}$ so that the three pairs of tests produced consistent results for T_i/T_{tot} and $I\Delta P_i$.

[33] Figure 7 shows the best model fit to the subset of FFEC profiles that are amenable to analysis. The first profile shown for each test was used as the model initial condition, and as shown in Figure 4, this was the first profile collected after Q became constant. The deepest peak, barely visible at 438 m depth, was not analyzed, as it does not evolve like a peak caused by a normal inflow point. This peak may be caused by the drilling sludge at the bottom of the wellbore. The next three distinct peaks (depths of 350, 280, and 220 m) show classic growing and skewing behavior. Within a given test (e.g., Figure 7a), upward flow within the borehole ("upflow") increases as one moves up the borehole, so peak skewing increases, with the upgradient (deeper) limb of the peak becoming steeper and the downgradient (shallower) limb of the peak becoming flatter. Comparing tests with successively greater pumping rates (e.g., Figures 7a–7c, peak at 280 m) shows the same pattern: As pumping rate increases, upflow increases and peak skewing increases. The model matches for all these peaks are very good, and the distinctive dependence of peak features on upflow means that the corresponding estimates for feed point strengths are well constrained.

[34] Another unknown parameter that was determined by trial and error along with the q_i and C_i values is the solute dispersion coefficient in the borehole. Because the FEC probe moves up and down the well, and the well is being pumped, this dispersion coefficient is generally several orders of magnitude bigger than the molecular diffusion coefficient. We obtained a value of 0.004 m^2/s for the dispersion coefficient. Despite the common conceptual model that dispersion coefficient should increase with fluid

Table 1. Q, Q_{wb}, and Q_{form} for the Various Tests[a]

	Q (L/min)	Q_{wb} (L/min)	Q_{form} (L/min)	Σq_i (L/min)	Comment
Shallow tests	2	0.69	1.31	1.31	Σq_i unreliable because q of shallowest peak cannot be determined accurately
	10	5.82	4.18	4.18	
	19.1	12.76	6.34	6.34	
Deep tests	5	1.66	3.34	2.04	Σq_i much less than Q_{form}
	10	3.16	6.84	3.90	
	15	7.15	7.85	5.12	

[a]In each case, $Q_{\text{form}} = Q - Q_{wb}$, with Q_{wb} determined from the slope of the linear fits to water level versus time data shown in Figures 4 and 6.

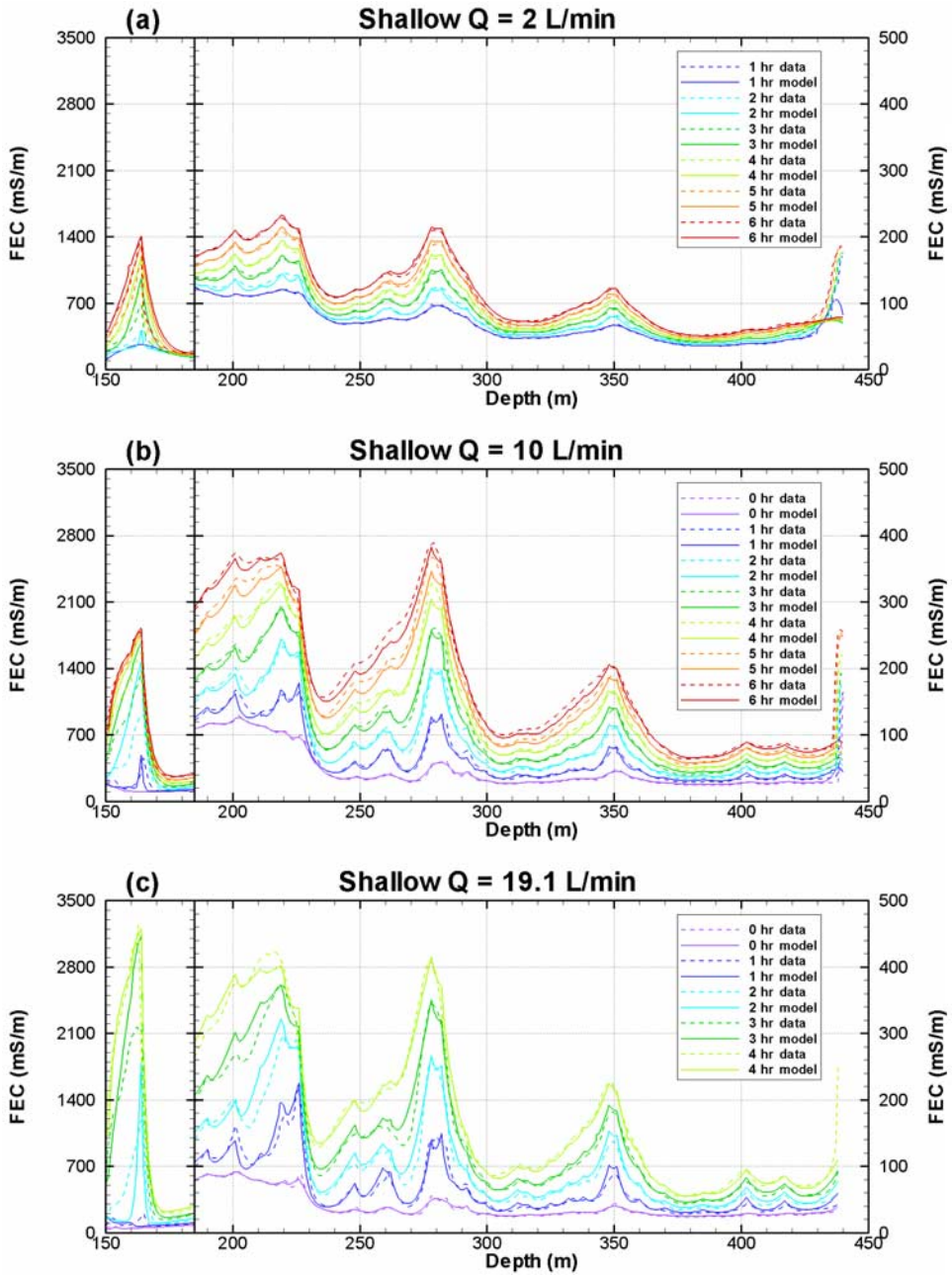

Figure 7. Processed FFEC data and model fit for shallow-zone tests. Note the different vertical scales for different depth ranges.

velocity, we found no need to use a velocity-dependent dispersion coefficient, either for different depth ranges within a single test or for tests with different pumping rates.

[35] The largest, shallowest peak at 164 m shows very little upflow (Figure 7), in fact, significantly less than the upflow shown by the smaller, deeper peaks. The upgradient limb of this peak is steep, consistent with the upflow inferred by matching the deeper peaks. However, the downgradient limb of this peak is not as flat as would be expected for continued upflow. This suggests that there is either an outflow just above the large, shallow peak, or an inflow of low-salinity water there. One possibility is that low-salinity shallow groundwater got into fractures at this level during the recirculation operation and is moving back into the wellbore during logging. This situation is too complicated to model with any accuracy, so the large shallow peak was not included in the quantitative analysis, but we inferred from this behavior that its transmissivity is large and its inherent hydraulic head is low.

[36] An interesting observation from the FFEC logs that has not been seen in previous studies involving granitic rock [*Doughty et al.*, 2005] is that the FEC value grew uniformly in time where no discrete peaks were present (e.g., around 375 m depth in Figure 7). One possibility is that water was flowing slowly into the wellbore through unfractured portions of mudstone rock matrix. The hydraulic conductivity

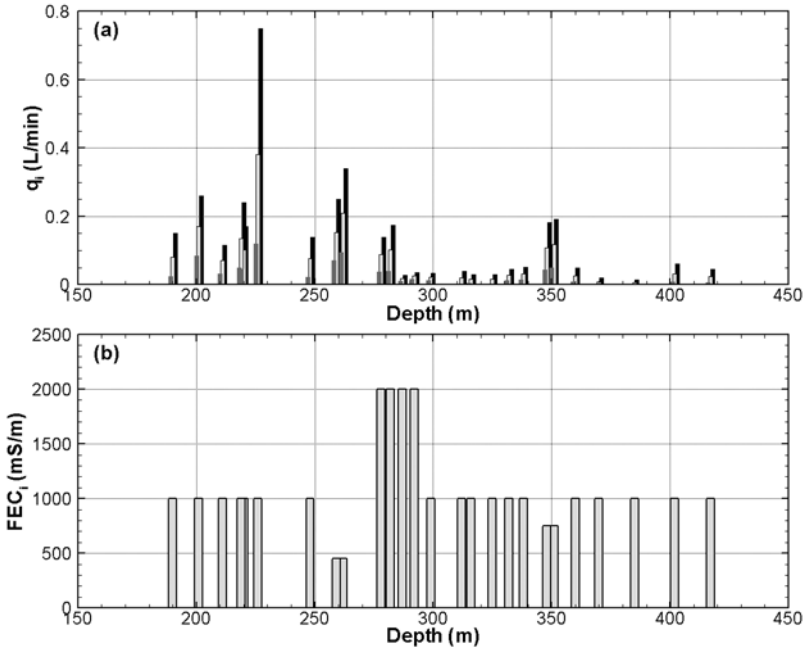

Figure 8. Direct-fit results for shallow-zone tests: (a) feed point strength q_i and (b) salinity (expressed as FEC in mS/m).

of intact mudstone at the Horonobe URL site has been estimated to be 100–10,000 times lower than the hydraulic conductivity of fractures and fracture zones [*Shigeta et al.*, 2003]. To simulate this formation flow, we introduced numerous tiny feed points distributed uniformly along the wellbore, all with the same q_i and C_i values. The q_i values were then varied in concert to match the portion of FFEC profiles where no discrete peaks exist. Another possibility is that the wellbore walls were coated with drilling mud, which contains salt that diffused into the wellbore fluid, causing a small FEC increase all along the borehole interval without the inflow of any formation fluid. To simulate this effect, we maintained the same q_iC_i product for the tiny points but increased C_i and decreased q_i by several orders of magnitude so that q_i would be small enough to have a negligible effect on flow up the wellbore. Both these approaches resulted in a slightly improved match to the shallow FFEC profiles, but the derived parameters q_i and C_i for the FEC peaks were not significantly changed. In conclusion, for this particular data set, the discrete FEC peaks are large enough so that any matrix flow or diffusion effect can be neglected.

[37] The direct-fit results for the shallow-zone tests are shown in Figure 8. Note that the C_i values are presented with FEC units of mS/m and that the values of z_i and C_i are the same for the three tests; only the q_i values differ between the three tests. Comparison of the C_i values with salinity and electric resistivity values found in other HDB Wells in the area [*Yamamoto et al.*, 2002a, 2002b; *Hama et al.*, 2007] shows that the values of C_i obtained by FFEC logging are consistent with those obtained by independent measurements.

[38] The mass integral method provides a way to look at the overall behavior of all the fractures intersecting the wellbore at one time, and can provide useful information for helping the FFEC log fitting process. In the mass integral method, each $C(z)$ profile is integrated over the depth interval of interest to obtain the area $A(t)$ under the $C(z)$ profile at time t. Then, $A(t)$ is multiplied by the mean wellbore cross-sectional area to determine ion mass in place at time t, which is denoted the mass integral $M(t)$ (for the present study, with C represented in FEC units mS/m rather than a salinity unit g/L, $M(t)$ is not a true mass, but the principle remains the same). If peaks reach the upper limit of the integration, a correction factor is introduced to account for mass being lost from the system, enabling subsections of the logged interval to be examined. Figure 9 shows a schematic diagram of three $M(t)$ integrals for the depth interval between 500 and 750 m.

[39] A plot of $M(t)$ versus t will be linear if mass is being added to the wellbore fluid at a constant rate, which will occur if q_i and C_i do not vary in time for any feed points, and additionally if all feed points are inflow points. Thus deviations of $M(t)$ from linearity provide information on the validity of model assumptions. If $M(t)$ is concave up, it

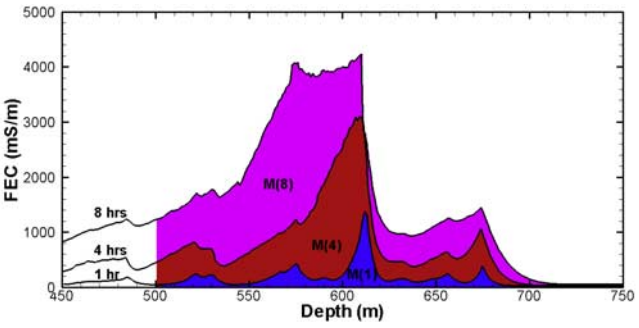

Figure 9. Schematic of the mass integral method for the depth interval 500–750 m.

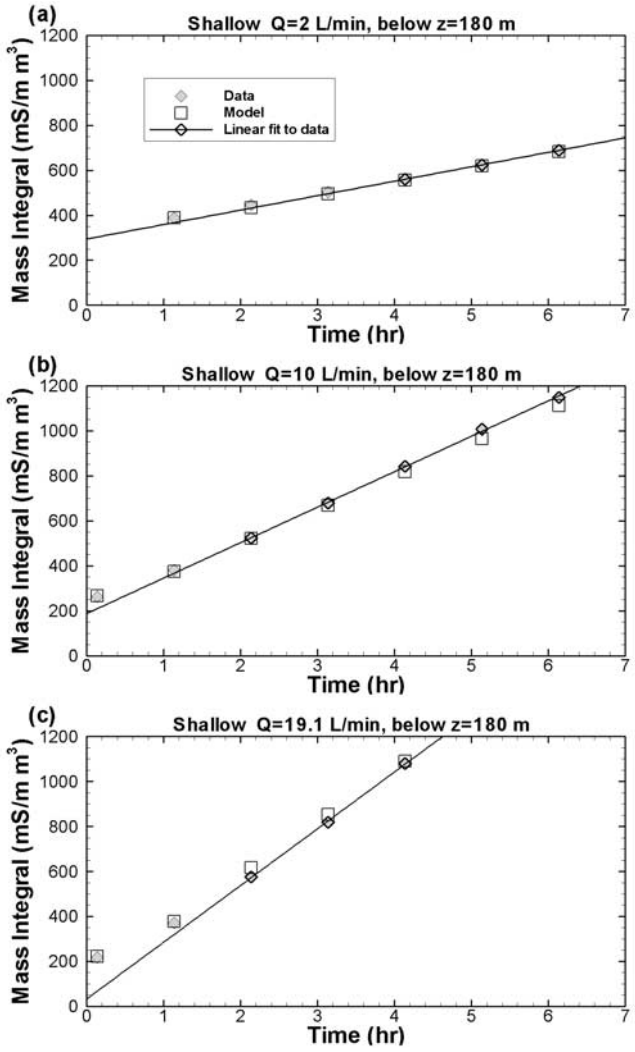

Figure 10. Mass integral results for shallow-zone tests. Each symbol represents integration of one FFEC profile. The first FFEC profile shown is used as the model initial condition for each test.

indicates that either q_i increases in time (a transient response to pumping) and/or that C_i increases in time (low-salinity shallow groundwater moved into fractures during recirculation so that during pumping inflow begins with low C_i values and increases to formation-water value). In contrast, if $M(t)$ is concave down, it suggests that q_i decreases in time or that outflow points are present.

[40] Figure 10 show the $M(t)$ versus t plots for the shallow-zone logs between depths of 180 and 440 m (i.e., the largest, shallowest peak at 164 m is excluded). For each test, $M(0) > 0$, indicating that there is a small amount of formation fluid in the wellbore at the start of logging, consistent with Figure 3. It is of interest to note that $M(0)$ differs between the three tests, suggesting different wellbore pressure conditions prevailed during the three recirculation periods. For each test, $M(t)$ is slightly concave up at early times, which we interpreted as representing the early time production of low-salinity shallow groundwater that had moved into the fractures during recirculation. The model was able to reproduce this behavior, despite assuming constant C_i values, by using a starting time $t_{0i} > 0$ at which each feed point begins to have a nonzero value of C_i. In order to obtain more accurate results from the fitting process, we focused on FFEC profiles collected during the period when $M(t)$ is linear. Generally, the agreement between the model and field values of $M(t)$ is very good, providing additional confidence in the fitting method.

[41] Results of the multirate analysis are shown in Figure 11 and Table 2. A total of 26 feed points were identified between depths of 180 and 420 m. Figure 11 shows that there is good consistency between T_i/T_{tot} and $I\Delta P_i$ values obtained using results of three different pairs of tests. Coupled with the good matches to the FFEC profiles themselves (Figure 7), and the fact that the feed point salinities are all within the range shown for other HDB wells in the area [*Yamamoto et al.*, 2002a, 2002b; *Hama et al.*, 2007], this consistency provides a measure of confidence in the correctness of the FFEC-analysis results.

5. Analysis of Deep FFEC Logs

[42] Because the water level declines for the deep-zone tests (Figure 6) are not linear, the mass integral analysis was done for the deep-zone tests prior to direct fitting, to provide guidance on which profiles may be most amenable to analysis. Results are shown in Figure 12. All $M(t)$ profiles are concave up at early times, suggesting that consistent with the water level data, Q_{wb} was decreasing in time and Q_{form} was increasing. Additionally, there is the possibility that early time $C_i(t)$ was affected by low-salinity shallow groundwater that moved into the fractures during recirculation. Thus the late-time profiles, obtained when $M(t)$ is more linear, were emphasized in the fitting process. The FFEC profiles used for the model initial condition for each test are identified in Figure 12. Initial conditions were chosen so that the model period corresponds to the time period when $M(t)$ and water level decline (Figure 8) are linear.

[43] Matching the FFEC profiles for the deep-zone logs followed the same procedure as for the shallow-zone logs (described in the first paragraph of section 4). The initial trial assumed that all feed points had the same salinity (corresponding to 3000 mS/m). During the matching process, variable C_i values were introduced as needed to improve the match. For the dispersion coefficient, a value of 0.005 m^2/s was obtained, nearly the same as for the shallow zone.

[44] The FFEC profiles used for the analysis and the best model fit are shown in Figure 13. The match is excellent for the peaks below 620 m. The match for the large peaks at 603 m and 611 m is not quite as good, and this error propagates upward, making the matches for peaks above 600 m somewhat worse as well. Results for depths above 540 m are less certain because of the wellbore diameter change. Direct-fitting results of the individual tests are shown in Figure 14. Mass integral results for the best model (not shown) match the observed $M(t)$ data shown in Figure 12 very well; the model symbol would overlap at least half of observed symbol for all points. Multirate results are shown in Figure 15 and Table 3. A total of 18 deep feed points are identified.

[45] It is interesting to note from Table 1 that the sum of the feed point strengths Σq_i is significantly less than Q_{form}. This could be partly attributable to the diameter change, but

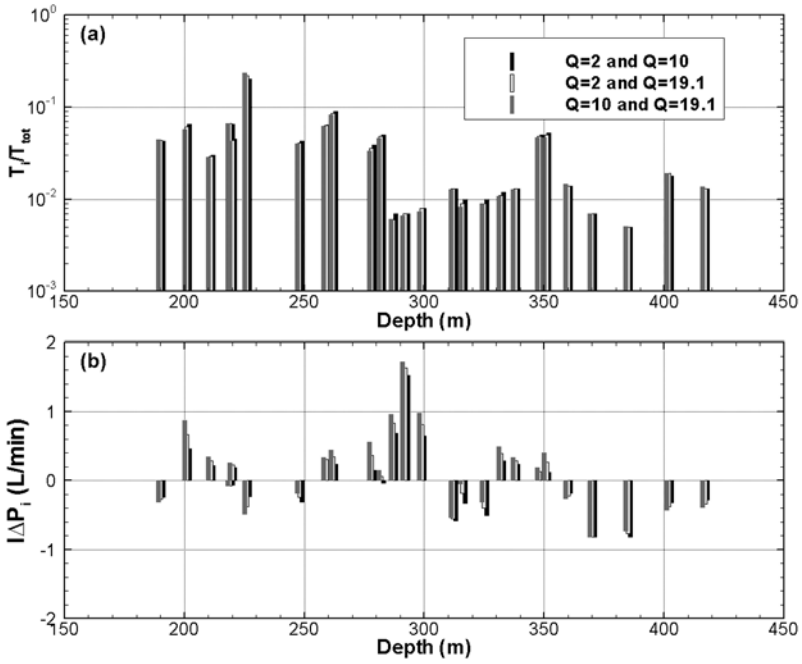

Figure 11. Multirate results for shallow-zone tests: (a) T_i/T_{tot} and (b) $I\Delta P_i$.

calculations indicated that the magnitude of the diameter change is not nearly big enough to account for the whole discrepancy. A bigger issue is the uncertainty in Q_{form} itself. In a sensitivity study, we found that if the q_i values were increased enough so that $\Sigma q_i = Q_{\text{form}}$, the resulting FFEC profiles showed far too much upflow. Therefore we hypothesize Q_{form} cannot be determined as $Q - Q_{wb}$, and that fluid is entering the wellbore above the logged interval, a phenomenon that has been noted at other sites [e.g., *Karasaki et al.*, 2000].

6. Comparison With Packer Test Results

[46] During the surface-based investigations (phase 1) of the Horonobe URL project, conducted between years 2000 and 2005, a total of 11 deep boreholes (HDB-1 through HDB-11) were drilled for an underground investigation of the geological environment in and around the main URL area at Horonobe. Well HDB-11, the deepest borehole (1020 m) in the URL area, was drilled during 2005 and 2006. A sequential approach to hydraulic testing was used at Well HDB-11, in which packer inflation, shut-in, pressure recovery, pulse test, slug test, long-term pumping test, and packer deflation were sequentially conducted in each of 10 packed-off intervals. The transient pressure responses to the multiple testing events in each interval were measured. In order to calculate hydraulic parameters such as transmissivity, hydraulic conductivity, storativity, and specific storage for each interval, standard analysis methods assuming radial flow geometry, such as those of *Cooper et al.* [1967], *Agarwal* [1980], *Hvorslev* [1951], and *Jacob* [1947], were applied to the pressure-transient data. Then the best fit parameters were selected as the representative values. Table 4 summarizes the depths, estimated transmissivities, and static hydraulic heads of the packed-off intervals, and the analysis methods used for the successful tests.

[47] Packer test results were made available to us after the conclusion of our FFEC analyses. They provide transmissivity and inherent hydraulic head values for seven 10–80 m intervals along the borehole where FFEC logging was done (Figure 16). In order to compare FFEC analysis results for the normalized transmissivity of fracture i, T_i/T_{tot}, to packer test results for transmissivity of interval L, $T_{L\text{-}pt}$, individual values of T_i/T_{tot} were summed over the depth intervals of the packer tests to obtain $T_{L\text{-}fec}$. Recall that transmissivity T (m^2/s) is an extrinsic property (it is proportional to the product of intrinsic permeability and a

Table 2. Multirate Analysis Results for Shallow-Zone Tests

Peak Number	Depth (m)	C_i (mS/m)	T_i/T_{tot}	$I\Delta P_i$ (L/min)
1	417	1000	0.013	−0.34
2	402	1000	0.019	−0.38
3	385	1000	0.005	−0.77
4	370	1000	0.007	−0.82
5	360	1000	0.014	−0.22
6	351	750	0.050	0.27
7	348	750	0.048	0.13
8	338	1000	0.013	0.29
9	332	1000	0.011	0.39
10	325	1000	0.009	−0.40
11	316	1000	0.009	−0.19
12	312	1000	0.013	−0.55
13	299	1000	0.008	0.81
14	292	2000	0.007	1.63
15	287	2000	0.006	0.83
16	282	2000	0.048	0.06
17	278	2000	0.036	0.36
18	262	450	0.086	0.34
19	259	450	0.063	0.31
20	248	1000	0.041	−0.24
21	226	1000	0.221	−0.38
22	220	1000	0.044	0.22
23	219	1000	0.067	−0.08
24	211	1000	0.029	0.28
25	201	1000	0.061	0.67
26	190	1000	0.044	−0.28

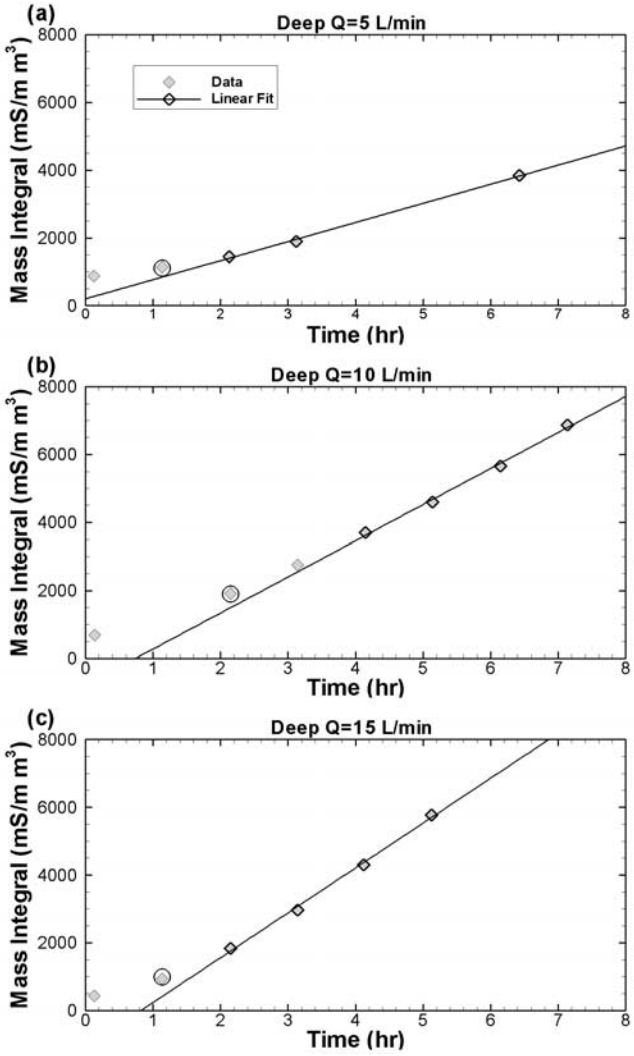

Figure 12. Mass integral results for deep-zone tests. Each symbol represents integration of one FFEC profile. The FFEC profile used as the model initial condition is circled.

thickness), so simply summing over T_i produces T_L, and there is no need to weigh different T_i values by fracture aperture or be concerned with fracture spacing. For the Lth interval,

$$T_{L-fec} = \sum_{i \subset L} T_i = T_{\text{tot}} \sum_{i \subset L} \left(\frac{T_i}{T_{\text{tot}}} \right). \tag{4}$$

[48] The introduction of T_{tot} on the far right-hand side is required because FFEC analysis just provides the ratio of transmissivities (T_i/T_{tot}), not the absolute transmissivity value T_i. Recall that T_{tot} is the total transmissivity of the borehole interval that is open during logging. In the present case, there are no reliable measurements to provide T_{tot}, so it was inferred to be the value which sets

$$\sum_L T_{L-fec} = \sum_L T_{L-pt}$$

within each zone. The resulting values of T_{tot} for the shallow and deep zones are presented in Table 5.

[49] The average inherent hydraulic head of interval L is denoted P_L. The value measured by the packer tests is denoted $P_{L\text{-}pt}$. The value determined by FFEC logging is denoted $P_{L\text{-}fec}$, and is obtained by averaging over inherent head values of individual fractures P_i

$$P_{L-fec} = \frac{\sum_{i \subset L} P_i T_i}{T_{L-fec}}. \tag{5}$$

However, because the multirate FFEC logging method does not determine the P_i values directly, but rather the $I\Delta P_i$ group given by equation (2), equation (5) does not provide a simple means for determining $P_{L\text{-}fec}$. The actual procedure used was to first rearrange equation (2) to provide an expression for P_i in terms of the outputs of a multirate FFEC analysis, P_{avg}, and I:

$$P_i = P_{\text{avg}} + \frac{Q_1}{T} \left(\frac{q_i^{(1)}/Q_1}{T_i/T_{\text{tot}}} - 1 \right). \tag{6}$$

Then, assuming that inflow strength and transmissivity are additive (i.e., that the fractures respond independently), a comparable expression was written for $P_{L\text{-}fec}$:

$$P_{L-fec} = P_{\text{avg}} + \frac{Q_1}{I} \left(\frac{\sum_{i \subset L} q_i^{(1)}/Q_1}{T_{L-fec}/T_{\text{tot}}} - 1 \right). \tag{7}$$

Recall that I is defined in equation (3) as the ratio of pumping rate Q to steady state drawdown ΔP for an open-borehole well test. For the present analysis, no independent well test was done, so the value of I had to be determined from water level data collected during FFEC logging (Figure 4 and Figure 6), for which neither Q nor ΔP can be determined unequivocally. For each zone, reasonably consistent values of I were obtained for the three tests, by extrapolating the late-time water level data to estimate ΔP and, for the deep zone, using the sum of the model values of q_i in place of Q. There is a significant degree of subjectivity in determining I, so there is a correspondingly large uncertainty in the resulting values of $P_{L\text{-}fec}$.

[50] Equation (7) indicates that the value of I controls the spread among $P_{L\text{-}fec}$ values for different L intervals and that P_{avg} simply provides a constant shift to the different $P_{L\text{-}fec}$ values. P_{avg} was inferred to be the value which sets

$$\sum_L P_{L-fec} = \sum_L P_{L-pt}$$

within each zone. The resulting values of P_{avg} for the shallow and deep zones are shown in Table 5.

[51] Figure 16 compares the transmissivities T_L and hydraulic heads P_L obtained from the packer tests with the results of the multirate analysis. Note that the deep logged interval extends to 775 m in depth, but no peaks develop below 700 m. This is consistent with the very low $T_{L\text{-}pt}$ value obtained for the 700–730 m depth interval, which is inferred to represent the unfractured rock matrix. For the shallow zone, the two $T_{L\text{-}pt}$ values are nearly the same, whereas the $T_{L\text{-}fec}$ values differ by about a factor of 2,

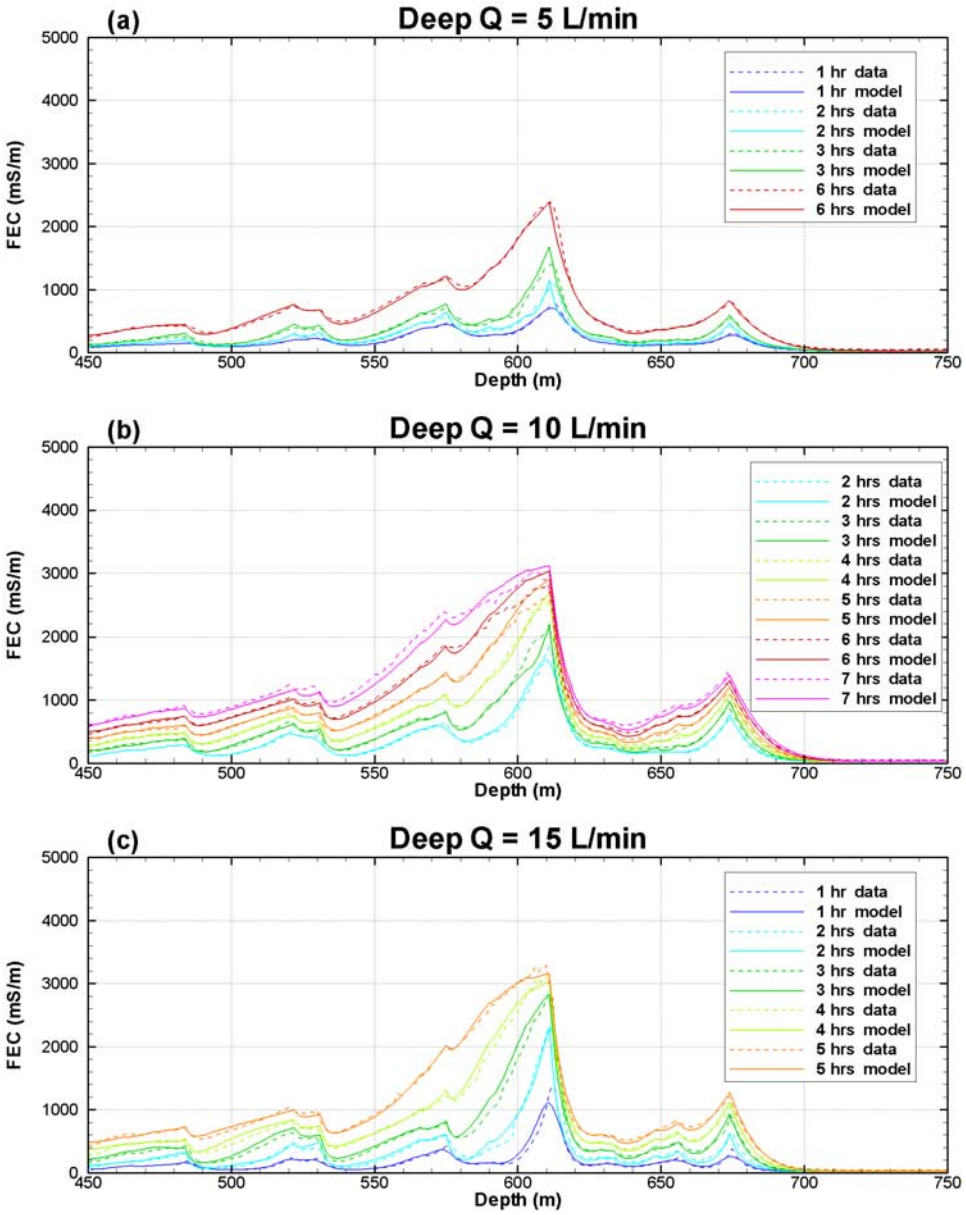

Figure 13. Processed FFEC data and model fit for deep-zone tests.

a reasonable agreement for fracture transmissivities, which can vary by orders of magnitude. For the deep zone, there are two $T_{L\text{-}pt}$ values shown for the depth interval 600–640 m. The larger one (from a slug test) is considered less reliable than the smaller one (from a long-term pumping test). The $T_{L\text{-}fec}$ and $T_{L\text{-}pt}$ values agree very well for the three intervals between 600 and 700 m depth. For the interval just above 600 m depth, $T_{L\text{-}pt}$ is again about a factor of 2 larger than $T_{L\text{-}fec}$. In this case, $T_{L\text{-}fec}$ may be the more accurate value, as it reflects flow through the permeable features at 565–585 m depth only. In contrast, $T_{L\text{-}pt}$ may reflect flow through the features at 565–585 m depth as well as flow from the higher-transmissivity interval at 600–640 m depth [*Doughty et al.*, 2005].

[52] Values of $P_{i\text{-}fec}$ are considered less reliable than $T_{L\text{-}fec}$ for two reasons. First, among the fundamental results of the matching process, $I\Delta P_i$ is less reliable than T_i/T_{tot} because, by nature of its more complicated functional form (compare equations (1) and (2)), $I\Delta P_i$ is more sensitive to small errors in q_i values than is T_i/T_{tot}. Second, the value of I used to convert $I\Delta P_i$ to P_{i} is highly uncertain, making $P_{L\text{-}fec}$ highly uncertain as well. With these caveats, the comparison of $P_{l\text{-}pt}$ and $P_{L\text{-}fec}$ shown in Figure 16 is considered reasonable. For the shallow zone, $P_{l\text{-}pt}$ values show more variability, whereas for the deep zone, $P_{L\text{-}fec}$ values show more variability, but the range of all the variations is relatively small, consistent with our findings from recirculation and logging initial conditions that internal wellbore flow is a minor effect.

7. Discussion

[53] In the present paper, we addressed a number of nonideal conditions that may be encountered in FFEC logging. In a system with a rapid hydrologic response, the

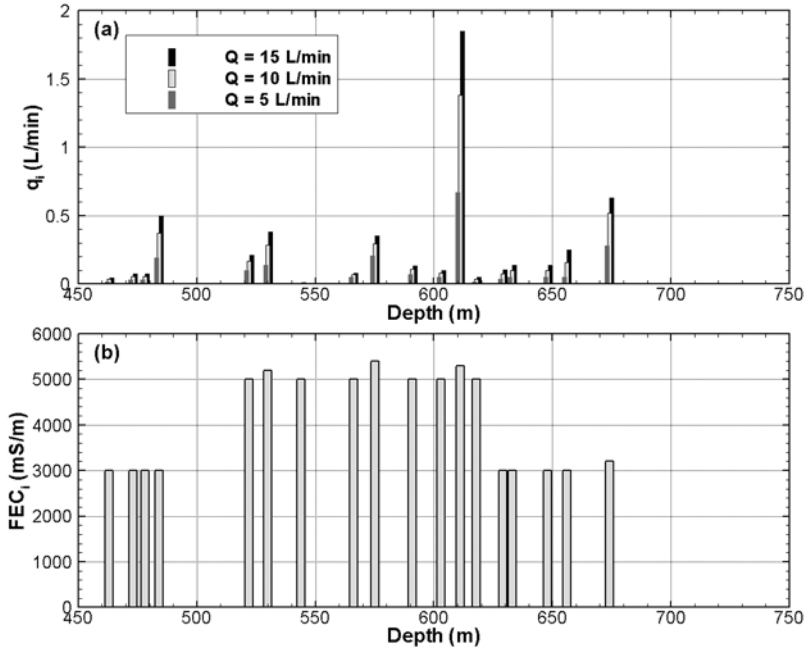

Figure 14. Direct-fit results for deep-zone tests: (a) feed point strength q_i and (b) salinity (expressed as FEC in mS/m).

water level in the borehole P_{wb} would drop quickly in response to the onset of pumping, and remain at a steady value thereafter. Thus after a short transient period, Q_{wb} would be zero and Q_{form} would equal the pumping rate Q, a constant, and the steady-flow assumption of BORE II would be met. We would then be well justified to use the difference between the unpumped water level P_{avg} and the pumped water level P_{wb} as part of the multirate analysis. The nonsteady water level observed during logging in the present set of measurements (Figure 4 and Figure 6) indicates that the hydrologic response of the system to the initiation of pumping was quite slow, and in fact water level changed throughout the logging period. This complicated several facets of the FFEC analysis. At a fundamental level, the assumption of steady state flow from the formation to the wellbore, Q_{form}, which BORE II relies on, may not be valid. Thus there was a need to determine which portions of the logging period were most amenable to analysis. For this, we used water level data and mass integral analysis to ascertain when Q_{form} was most constant: For a constant

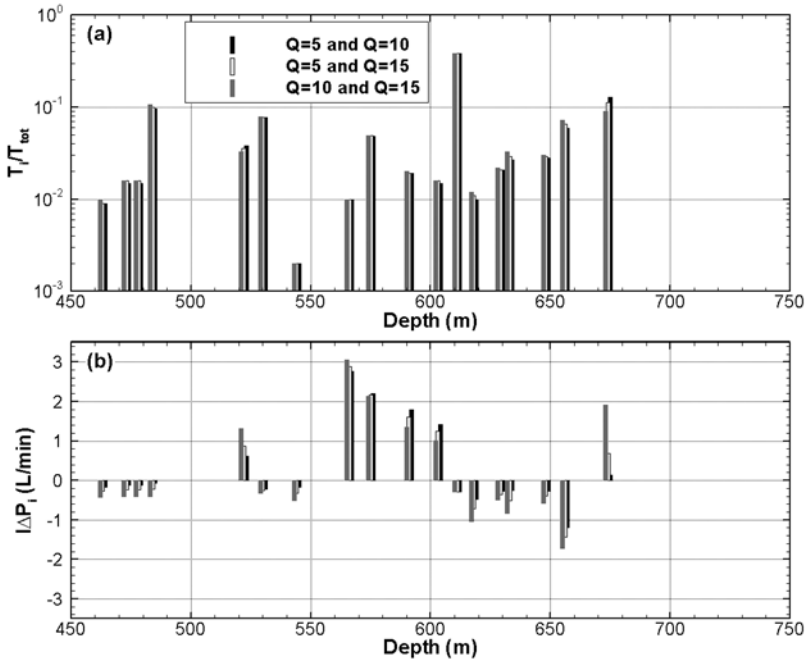

Figure 15. Multirate results for deep-zone tests: (a) T_i/T_{tot} and (b) $I\Delta P_i$.

Table 3. Multirate Analysis Results for Deep-Zone Tests

Peak Number	Depth (m)	C_i (mS/m)	T_i/T_{tot}	$I\Delta P_i$ (L/min)
1	674	3200	0.113	0.69
2	656	3000	0.065	−1.43
3	648	3000	0.029	−0.40
4	633	3000	0.029	−0.50
5	629	3000	0.021	−0.36
6	618	5000	0.011	−0.72
7	611	5300	0.382	−0.29
8	603	5000	0.016	1.25
9	591	5000	0.019	1.61
10	575	5400	0.049	2.18
11	566	5000	0.010	2.88
12	544	5000	0.002	−0.32
13	530	5200	0.078	−0.26
14	522	5000	0.036	0.88
15	484	3000	0.100	−0.21
16	478	3000	0.016	−0.23
17	473	3000	0.016	−0.23
18	463	3000	0.009	−0.28

pumping rate Q, a linearly declining water level implies a constant Q_{wb} and hence a constant Q_{form}; a linear $M(t)$ implies a constant Q_{form} and also constant C_i values. When Q_{form} was uncertain, the constraint on the q_i requiring $\Sigma q_i = Q_{\text{form}}$ had to be relaxed.

[54] Generally, with a slowly responding system, it is difficult to determine P_{wb}, and even difficult to ascertain whether the hydraulic head measured before pumping begins is truly representative of P_{avg}. An open-hole well test to determine T_{tot}, natural-state hydraulic head P_{avg}, and drawdown $P_{\text{avg}} - P_{wb}$ would remove some uncertainty. Such results would also be useful for comparing with FFEC results and to packer test results. *Paillet* [2004] has investigated difficulties associated with flow logging in slowly responding systems, and made several suggestions for ameliorating them. However, for the schedule required for FFEC logging, in which recirculation should take place with no hydraulic head change, followed immediately by logging, which must begin as soon as pumping is initiated to resolve early growth of FEC peaks, it is not clear if these suggestions can be applied.

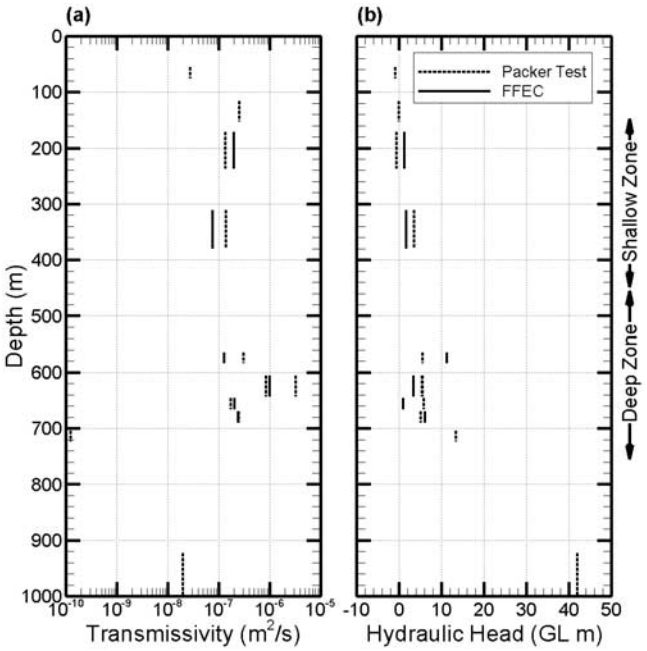

Figure 16. Comparison of packer test results and values inferred from multirate FFEC logging for (a) transmissivity and (b) hydraulic head for selected intervals in Well HDB-11.

[55] For Well HDB-11, the shallow-zone tests showed more linear water level declines than did the deep-zone tests, enabling Q_{form} to be ascertained with greater certainty. For the shallow-zone tests, a good match was obtained for all the small peaks. Only the uppermost, largest peak was not analyzable. It is fortunate that the peak that could not be analyzed is the shallowest peak, because as such it has no effect on any deeper peaks. Generally, any peaks occurring above a nonanalyzable peak would also be nonanalyzable.

[56] For the deep-zone tests, a reasonably good match was obtained for all the peaks, but the nonlinearity of the water level decline indicated that Q_{form} was not constant,

Table 4. Summary of Packer Test Results

Packed-Off Intervals					Test Results (Representative Values)		
Upper End (m bgs)[a]	Lower End (m bgs)	Interval Thickness (m)	Stratigraphy (Formation)	FFEC Logging Zone	Transmissivity (m^2/s)	Static Hydraulic head (m ags)[b]	Analysis Method
55.5	75.5	20	Koetoi		2.77E-08	−0.96	Agarwal
115	153	38	Koetoi		2.60E-07	−0.07	Cooper
171	237	66	Koetoi	shallow	1.37E-07	−0.70	Agarwal
311	380	69	Koetoi	shallow	1.40E-07	3.56	Cooper
564	584	20	Wakkanai	deep	3.07E-07	5.50	Cooper
606[c]	644	38	Wakkanai	deep	3.28E-06	5.57	Cooper
606[c]	644	38	Wakkanai	deep	8.63E-07	5.32	Jacob
646	666	20	Wakkanai	deep	1.76E-07	5.74	Cooper
670	690	20	Wakkanai	deep	2.51E-07	5.08	Cooper
704	724	20	Wakkanai	deep	1.25E-10	13.41	Agarwal
923	1000	77	Wakkanai		2.01E-08	41.98	Hvorslev

[a]Meters below ground surface.
[b]Meters above ground surface.
[c]The upper packer test labeled 606–644 shows the results of a slug test, while the lower test labeled 606–644 shows results of a long-term pumping test. Therefore the lower results are more reliable.

Table 5. Parameters Used for Comparison Between Results of Multirate Flowing FFEC Logging Analysis and Packer Tests

	Zone	
Parameter	Shallow	Deep
Depth (m)	150–450	450–775
T_{tot} (m^2/s)	4.3×10^{-7}	2.2×10^{-6}
I (m^2/s)	2.5×10^{-6}	5.5×10^{-6}
P_{avg} (m ags)[a]	1.5	5.9

[a]Meters above ground surface.

again precluding the constraint $\Sigma q_i = Q_{form}$ from being used. In fact, it was impossible to match the profiles unless $\Sigma q_i \ll Q_{form}$, suggesting that inflow to the well occurred above the depth interval that was logged.

[57] During the deep-zone matching procedure, it became apparent that the FFEC profiles could be equally well matched with alternative sets of salinity values. C_i values of 5000, 10,000, 15,000, or 25,000 mS/m could be assigned to feed points at depths around 600 m, and with suitable q_i choices all could produce reasonable matches to the observed FFEC profiles. This nonuniqueness points out the usefulness of independent information when applying the FFEC method. Figure 17 compares FEC obtained from groundwater squeezed from core samples obtained during the drilling of Well HDB-11 with the C_i values inferred from FFEC logging. There is not expected to be a one-to-one correspondence between the two independently obtained data sets, as core samples mainly contain groundwater held in the rock matrix, as opposed to FFEC analysis results, which reflect groundwater moving through fractures. Because matrix permeability is much smaller than fracture permeability, the spatial range that the electric conductivity values represent is quite different. However, because there is expected to be at least some communication between fracture and matrix fluids, core sample FEC values should be useful to constrain the order of magnitude of FFEC analysis values. Additionally, differences between core sample values and FFEC analysis values may indicate areas where fluid flow through fractures is significant.

[58] Figure 17 shows that core samples have a maximum FEC of 3500 mS/m. This certainly favors the FFEC analysis using C_i = 5000 mS/m for feed points at 600 m depth as opposed to the analyses using higher C_i values. FFEC matching was attempted using $C_i \approx 3500$ mS/m, consistent with the HDB-11 core sample values, but the model produced far too low a peak at a depth of 600 m, regardless of the q_i values chosen. Moreover, groundwater squeezed from core samples from Well HDB-1, located about 500 m NW of Well HDB-11, produced FEC values as high as 6000 mS/m for depths around 600 m [*Hama et al.*, 2007], corroborating the plausibility of the FFEC-analysis results.

[59] For the shallow zone, Figure 17 shows an increase in FEC at a depth of about 280 m in both data sets, but the FEC values used in the FFEC analysis are consistently smaller than the core sample values. FFEC matching was attempted using larger C_i values consistent with core sample results, but the correspondingly smaller q_i values produced far too small an upflow in the wellbore. Again, core samples from Well HDB-1 provide support for the use of smaller C_i values, showing FEC values around 1000 mS/m for depths of 300–400 m [*Hama et al.*, 2007].

8. Concluding Remarks

[60] In spite of the various complications associated with the test data described in the analysis sections above, the 6 days of FFEC logging have yielded internally consistent information on location, salinity, and transmissivity and inherent hydraulic heads of 44 conducting fractures. Data collection included 3 days of FFEC logging for the shallow zone (Koetoi formation, 150 to 450 m depth; Table 2) and 3 days of FFEC logging for the deep zone (Wakkanai formation, 450 to 775 m depth; Table 3). Among the results, location is determined unequivocally and transmissivity is considered to be well determined. Salinity and hydraulic head values are somewhat less certain, but the small variability among hydraulic head values makes the latter uncertainty of minimal importance.

[61] A careful study was made to compare the detailed results on these 44 conducting fractures with transmissivity and hydraulic head data obtained from packer tests for seven intervals with length ranging from 10 to 80 m. Overall, it has been shown that the FFEC logging results are consistent with these independent data. The success of the FFEC analysis method under these nonideal conditions provides evidence of the robustness of the method. Further, FFEC results provide more detailed information than packer tests, as they yield hydraulic properties of individual fractures rather than averaged properties of the intervals between packers.

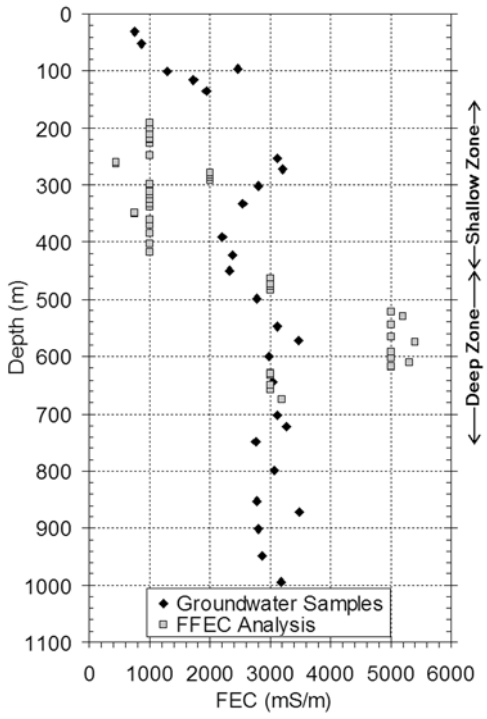

Figure 17. Comparison of FEC values inferred from FFEC logging and electric conductivity from groundwater squeezed from core samples from Well HDB-11.

[62] A number of further analyses are possible, in order to improve confidence in the results. We could specify time-dependent feed point strengths $q_i(t)$, to account for a time-dependent Q_{form}, and time-dependent feed point salinities $C_i(t)$, to account for the presence of low-salinity shallow groundwater water in the fractures at the onset of pumping. We could also model the recirculation period and the rest period between the end of the recirculation period and the onset of pumping as was done for the Tono FFEC logging analysis [*Doughty et al.*, 2005], in order to develop insight into internal flow and produce more accurate initial conditions for the logging period. For the deep-zone tests, we could try to account for the variable wellbore diameter. It may be possible to do this with fictitious outflow points as was done by *Doughty et al.* [2005] for a simple one-time change in borehole diameter. Another alternative would be to modify the BORE II code itself to enable variable borehole diameters to be considered.

[63] Concerning potential improvements of field test procedures for future FFEC logging applications, we make the following recommendations. If possible, do recirculation at a lower rate to maintain wellbore hydraulic head closer to P_{avg}, and thus, to minimize flow of low-salinity groundwater into fractures. Keep the pumping rate constant during logging, or at least measure rate changes if they are unavoidable. Continue logging until logs show evidence of the approach to steady state FFEC profiles (plateaus). Plateaus greatly reduce ambiguity in parameter choice for diffusion coefficient, q_i, C_i. Continue logging until water level in the wellbore is constant or linearly declining, to enable Q_{form} to be determined unambiguously. If possible, emplace a packer in the well just above the pump to avoid the problem of a declining water level in the well during pumping (i.e., setting $Q_{wb} = 0$). If a profile of FEC is distorted by muddy water adhering to a sensor, withdraw and clean the sensor and repeat the log. Obtain and use (at least) one salinity measurement at a deeper borehole inflow point in FFEC log analysis. This can greatly reduce the nonuniqueness inherent in matching peaks that do not move strongly up the well.

[64] **Acknowledgments.** We thank Kenzi Karasaki of Lawrence Berkeley National Laboratory and three anonymous reviewers for their careful reviews and helpful comments on this paper. This work was supported by the Japan Atomic Energy Agency (JAEA) under the Binational Research Cooperative Program between JAEA and the U.S. Department of Energy, Office of Civilian Radioactive Waste Management, Office of Science and Technology. The work was performed under the auspices of the U.S. Department of Energy through contract DE-AC02-05CH11231.

References

Agarwal, R. G. (1980), A new method to account for producing time effects when drawdown type curves are used to analyze pressure buildup and other test data, SPE paper 9289 presented at the 55th SPE Annual Technical Conference and Exhibition, Dallas, Tex., 21–24 Sept.

Bauer, G. D., and J. J. LoCoco (1996), Hydrogeophysics determines aquifer characteristics, *Int. Ground Water Technol.*, *2*, 12–16.

Brainerd, R. J., and G. A. Robbins (2004), A tracer dilution method for fracture characterization in bedrock wells, *Ground Water*, *42*(5), 774–780, doi:10.1111/j.1745-6584.2004.tb02731.x.

Cooper, H. H., J. D. Bredehoeft, and S. S. Papadopulos (1967), Response of a finite-diameter well to an instantaneous charge of water, *Water Resour. Res.*, *3*(1), 263–269, doi:10.1029/WR003i001p00263.

Doughty, C., and C.-F. Tsang (2000), BORE II—A code to compute dynamic wellbore electrical conductivity logs with multiple inflow/outflow points including the effects of horizontal flow across the well, *Rep. LBL-46833*, Lawrence Berkeley Natl. Lab., Berkeley, Calif.

Doughty, C., and C.-F. Tsang (2005), Signatures in flowing fluid electric conductivity logs, *J. Hydrol.*, *310*, 157–180, doi:10.1016/j.jhydrol.2004.12.003.

Doughty, C., S. Takeuchi, K. Amano, M. Shimo, and C.-F. Tsang (2005), Application of multirate flowing fluid electric conductivity logging method to well DH-2, Tono Site, Japan, *Water Resour. Res.*, *41*, W10401, doi:10.1029/2004WR003708.

Evans, D. G. (1995), Inverting fluid conductivity logs for fracture inflow parameters, *Water Resour. Res.*, *31*(12), 2905–2915, doi:10.1029/95WR02482.

Evans, D. G., W. P. Anderson Jr., and C.-F. Tsang (1992), Borehole fluid experiments near salt contamination sites in Maine, in *Proceedings of the NGWA Conference on Eastern Regional Ground Water Issues*, pp. 797–807, Natl. Ground Water Assoc., Westerville, Ohio.

Guyonnet, D., A. Rivera, S. Löw, and N. Correa (1993), Analysis and synthesis of fluid logging data from Wellenberg boreholes SB1, SB3, SB4 and SB6, *Nagra Tech. Rep., NTB 92–01*, 153 pp., Nagra, Wettington, Switzerland.

Hale, F. V., and C.-F. Tsang (1988), A code to compute borehole conductivity profiles from multiple feed points, *Rep. LBL-24928*, Lawrence Berkeley Natl. Lab., Berkeley, Calif.

Hale, F. V., and C.-F. Tsang (1994), VHBORE: A code to compute borehole fluid conductivity profiles with pressure changes in the borehole, *Rep. LBL-31050*, Lawrence Berkeley Natl. Lab., Berkeley, Calif.

Hama, K., T. Kunimaru, R. Metcalfe, and A. J. Martin (2007), The hydrogeochemistry of argillaceous rock formations at the Horonobe URL site, Japan, *Phys. Chem. Earth, Parts A, B, and C*, *32*(1–7), 170–180.

Hvorslev, M. J. (1951), Time lag and soil permeability in ground-water observations, *Bull. 36*, pp. 1–50, Waterways Exp. Stn., U.S. Army Corps of Eng., Vicksburg, Miss.

Jacob, C. E. (1947), Drawdown test to determine effective radius of artesian well, *Trans. Am. Soc. Civ. Eng.*, *112*, 1047–1064.

Karasaki, K., B. Freifeld, A. Cohen, K. Grossenbacher, P. Cook, and D. Vasco (2000), A multidisciplinary fractured rock characterization study at Raymond field site, Raymond, CA, *J. Hydrol.*, *236*, 17–34, doi:10.1016/S0022-1694(00)00272-9.

Kelley, V. A., J. M. Lavanchy, and S. W. Löw (1991), Transmissivities and heads derived from detailed analysis of Siblingen 1989 fluid logging data, *Nagra Tech. Rep., NTB 90–09*, 184 pp., Nagra, Wettington, Switzerland.

Löw, S., V. Kelley, and S. Vomvoris (1994), Hydraulic borehole characterization through the application of moment methods to fluid conductivity logs, *J. Appl. Geophys.*, *31*(1–4), 117–131, doi:10.1016/0926-9851(94)90051-5.

Marschall, P., and S. Vomvoris (Eds.) (1995), Grimsel Test Site: Developments in hydrotesting, fluid logging and combined salt/heat tracer experiments in the BK Site (Phase III), *Nagra Tech. Rep. 93–47*, Nagra, Wettingen, Switzerland.

Molz, F. J., R. H. Morin, A. E. Hess, J. G. Melville, and O. Guven (1989), The impeller meter for measuring aquifer permeability variations: Evaluation and comparison with other tests, *Water Resour. Res.*, *25*(7), 1677–1683, doi:10.1029/WR025i007p01677.

Öhberg, A., and P. Rouhiainen (2000), Groundwater flow measuring techniques, *Posiva 2000–12*, Posiva Oy, Helsinki, Finland.

Paillet, F. L. (1998), Flow modeling and permeability estimation using borehole flow logs in heterogeneous fractured formations, *Water Resour. Res.*, *34*(5), 997–1010, doi:10.1029/98WR00268.

Paillet, F. L. (2000), A field technique for estimating aquifer parameters using flow log data, *Ground Water*, *38*(4), 510–521, doi:10.1111/j.1745-6584.2000.tb00243.x.

Paillet, F. (2004), Borehole flowmeter applications in irregular and large-diameter boreholes, *J. Appl. Geophys.*, *55*, 39–59, doi:10.1016/j.jappgeo.2003.06.004.

Paillet, F. L., and W. H. Pedler (1996), Integrated borehole logging methods for wellhead protection applications, *Eng. Geol.*, *42*(2–3), 155–165, doi:10.1016/0013-7952(95)00077-1.

Pedler, W. H., C. L. Head, and L. L. Williams (1992), Hydrophysical logging: A new wellbore technology for hydrogeologic and contaminant characterization of aquifers, paper presented at the National Outdoor Action Conference, Natl. Ground Water Assoc., Las Vegas, Nev., 11–13 May.

Schlumberger, Ltd. (1984), Log interpretation charts, New York.

Shigeta, N., S. Takeda, H. Matsui, and S. Hamasaki (2003), Underground research laboratories for crystalline rock and sedimentary rock in Japan, paper presented at the Waste Management 2003 Conference, WM Symposia, Inc., Tucson, Ariz, 23–27 Feb.

Tsang, C.-F., and C. Doughty (2003), Multirate flowing fluid electric conductivity logging method, *Water Resour. Res.*, *39*(12), 1354, doi:10.1029/2003WR002308.

Tsang, C.-F., P. Hufschmied, and F. V. Hale (1990), Determination of fracture inflow parameters with a borehole fluid conductivity logging method, *Water Resour. Res.*, *26*(4), 561–578.

Yamamoto, T., M. Shimo, Y. Fujiwara, H. Hattori, T. Tadokoro, H. Iwama, M. Nago, and S. Kumamoto (2002a), HDB-1 borehole investigations in Horonobe Underground Research Center (in Japanese), *Rep. JNC TJ1400 2002–010*, Jpn. At. Energy Agency, Tokaimura, Japan.

Yamamoto, T., M. Shimo, Y. Fujiwara, H. Hattori, T. Tadokoro, H. Iwama, M. Nago, and S. Kumamoto (2002b), HDB-2 borehole investigations in Horonobe Underground Research Center (in Japanese), *Rep. JNC TJ1400 2002–011*, Jpn. At. Energy Agency, Tokaimura, Japan.

C. Doughty and C.-F. Tsang, Earth Sciences Division, Lawrence Berkeley National Laboratory, Berkeley, CA 94720, USA. (cadoughty@lbl.gov)

K. Hatanaka and S. Yabuuchi, Horonobe Underground Research Unit, Japan Atomic Energy Agency, Horonobe-cho, Teshio-gun, Hokkaido, 098-3224, Japan.

H. Kurikami, Nuclear Waste Management Organization of Japan, 1-23, Shiba 4-chome, Minato-ku, Tokyo 108-0014, Japan.